

# Journal of Visualized Experiments

## In Situ Surface Temperature Measurement in a Conveyor Belt Furnace via Inline Infrared Thermography --Manuscript Draft--

Article Type:	Invited Methods Article - JoVE Produced Video
Manuscript Number:	JoVE60963R3
Full Title:	In Situ Surface Temperature Measurement in a Conveyor Belt Furnace via Inline Infrared Thermography
Section/Category:	JoVE Engineering
Keywords:	Infrared thermography; conveyor belt furnace; silicon solar cells; spatial temperature distribution; contact firing; quality assurance
Corresponding Author:	Daniel Ourinson Fraunhofer-Institut für Solare Energiesysteme Freiburg, Baden-Württemberg GERMANY
Corresponding Author's Institution:	Fraunhofer-Institut für Solare Energiesysteme
Corresponding Author E-Mail:	daniel.ourinson@ise.fraunhofer.de
Order of Authors:	Daniel Ourinson Gernot Emanuel Gunnar Dammaß Harald Müller Florian Clement Stefan W. Glunz
Additional Information:	
Question	Response
Please indicate whether this article will be Standard Access or Open Access.	Standard Access (US\$2,400)
Please indicate the <b>city, state/province, and country</b> where this article will be <b>filmed</b> . Please do not use abbreviations.	Freiburg

Dear Editor,

please find our manuscript with the title “In Situ Surface Temperature Measurement in a Conveyor Belt Furnace via Inline Infrared Thermography” attached. It covers methods how to install a thermography system into a conveyor belt furnace, how to conduct a customer correction of a factory calibrated infrared camera and how to perform the evaluation of the spatial surface temperature distribution on the targeted object.

Best regards,

Daniel Ourinson

**TITLE:**

**In Situ Surface Temperature Measurement in a Conveyor Belt Furnace via Inline Infrared Thermography**

**AUTHORS AND AFFILIATIONS:**

Daniel Ourinson<sup>1</sup>, Gernot Emanuel<sup>1</sup>, Gunnar Dammaß<sup>2</sup>, Harald Müller<sup>3</sup>, Florian Clement<sup>1</sup>, Stefan W. Glunz<sup>1</sup>

<sup>1</sup>Fraunhofer Institute for Solar Energy Systems ISE, Freiburg, Germany

<sup>2</sup>InfraTec GmbH, Gostritzer Straße 61-63, Dresden, Germany

<sup>3</sup>Rehm Thermal Systems GmbH, Blaubeuren-Seissen, Germany

**Corresponding Author:**

Daniel Ourinson (daniel.ourinson@ise.fraunhofer.de)

**Email Addresses of Co-Authors:**

Gernot Emanuel (gernot.emanuel@ise.fraunhofer.de)

Gunnar Dammaß (g.damass@infratec.de)

Harald Müller (h.mueller@rehm-group.com)

Florian Clement (florian.clement@ise.fraunhofer.de)

Stefan W. Glunz (stefan.glunz@ise.fraunhofer.de)

**KEYWORDS:**

infrared thermography, conveyor belt furnace, silicon solar cells, spatial temperature distribution, contact firing, quality assurance

**SUMMARY:**

This protocol describes how to install an infrared camera into a conveyor belt furnace, conduct a customer correction of a factory calibrated IR camera, and evaluate the spatial surface temperature distribution of an object of interest. The example objects are industrial silicon solar cells.

**ABSTRACT:**

Measuring the surface temperature of objects that are processed in conveyor belt furnaces is an important tool in process control and quality assurance. Currently, the surface temperature of objects processed in conveyor belt furnaces is typically measured via thermocouples. However, infrared (IR) thermography presents multiple advantages compared to thermocouple measurements, as it is a contactless, real-time, and spatially resolved method. Here, as a representative proof-of-concept example, an inline thermography system is successfully installed into an IR lamp powered solar firing furnace, which is used for the contact firing process of industrial Si solar cells. This protocol describes how to install an IR camera into a conveyor belt furnace, conduct a customer correction of a factory calibrated IR camera, and perform the evaluation of spatial surface temperature distribution on a target object.

## INTRODUCTION:

Process control and quality assurance of objects processed in conveyor belt furnaces<sup>1</sup> is important and accomplished by measuring the surface temperature of the object. Currently, the temperature is typically measured by a thermocouple<sup>1</sup>. As thermocouple measurements require contact with the object, thermocouples inevitably damage the object. Therefore, it is common to choose representative samples of a batch for temperature measurements, which are not further processed since they become damaged. The measured temperatures of these damaged objects are then generalized to the remaining samples from the batch, which are further processed. Accordingly, production must be interrupted for thermocouple measurements. Furthermore, the contact is local, needs to be readjusted after each measurement, and influences the local temperature, which makes these measurements time-intensive.

Infrared (IR) thermography<sup>2</sup> has a number of advantages over classic thermocouple measurements and represents a contactless, in-situ, real-time, time-saving, and spatially resolved temperature measurement method. Using this method, each sample of the batch, including those that are further processed, can be measured without interrupting production. In addition, the surface temperature distribution can be measured, which provides insight into temperature homogeneity during the process. The real-time feature allows correction of temperature settings on-the-fly. So far, the possible reasons for not using IR thermography in conveyor belt furnaces are 1) unknown optical parameters of hot objects (especially for nonmetals<sup>3</sup>) and 2) parasitic environmental radiation in the furnace (i.e., reflected radiation detected by the IR camera in addition to the emitted radiation from the object), which leads to false temperature output<sup>2</sup>.

Here, as a representative proof-of-concept example of IR thermography in a conveyor belt furnace, we successfully install an inline thermography system into an IR lamp powered solar firing furnace (**Figure 1**), which is used during the contact firing process of industrial Si solar cells (**Figure 2A,B**)<sup>4,5</sup>. The firing process is a crucial step at the end of industrial solar cell production<sup>6</sup>. During this step, the contacts of the cell are formed<sup>7,8</sup>, and surface passivation is activated<sup>9</sup>. To successfully achieve the latter, the time-temperature profile during the firing process (**Figure 2C**) must be accurately realized. Therefore, sufficient and efficient temperature control is required. This protocol describes how to install an IR camera into a conveyor belt furnace, conduct a customer correction of a factory calibrated IR camera, and evaluate the spatial surface temperature distribution of a target object.

## PROTOCOL:

### 1. Installation of IR camera into a conveyor belt furnace

1.1. Decide which part of the furnace should be measured by the IR camera.

NOTE: Here, the peak zone of the firing process is chosen (see the orange highlighted zone in the firing area of **Figure 1A**, which is zoomed in in **Figure 1B**).

1.2. Define the temperature range of interest that the IR camera should detect (e.g., 700–900 °C, the typical peak temperature range of the firing process).

1.3. Determine, or at least estimate (through experiments or literature), the temperature and spectral and angular dependent emissions of the object(s) of interest (e.g., silicon solar cell) to identify the wavelength range(s) of highest emission for the temperature range of interest (under a specific camera angle).

NOTE: Here, the emission is estimated based on previous literature<sup>3</sup> and a software called RadPro<sup>10</sup>, which calculates the spectral, angular, and temperature-dependent emissivity for certain materials (i.e., Si and Al layers).

#### 1.4. Deciding on the IR camera type

NOTE: Here, a midwave infrared (MWIR) indium antimonide (InSb) camera (**Table of Materials**) is used.

1.4.1. Choose a camera that can detect the temperature range of interest.

1.4.2. Select a camera whose detection wavelength range matches the wavelength range of highest emission of the object of interest in the temperature range of interest.

1.4.3. Avoid as much parasitic radiation detection by the camera as possible by avoiding objects that emit or reflect radiation into the camera field of view (e.g., IR lamps in a furnace).

1.4.4. Decide on the necessary spatial and temporal resolution of the camera (e.g., 640 px x 512 px and 125 Hz [full image] for the used camera here).

1.5. Realize a sufficient optical path from the IR camera to object (see **Figure 1B**).

1.5.1. Avoid disturbing objects in the optical path (e.g., IR lamps causing direct or reflected light).

1.5.2. Position the camera outside of the furnace chamber, if possible.

NOTE: Most cameras have low operating temperatures (e.g., up to 50 °C). Make sure in advance that the camera position can be changed, if desired.

1.5.3. Remove the furnace wall and isolation at the location where the optical path should be and replace the hole with an insulating IR window.

1.5.3.1. Choose the appropriate material for the window that meets the following demands: 1) as transparent as possible for the detection wavelength ( $\lambda$ ) range of the camera (e.g., quartz glass window for  $\sim 0.2 \mu\text{m} < \lambda < 3 \mu\text{m}$ , sapphire window for  $\sim 0.4 \mu\text{m} < \lambda < 4.2 \mu\text{m}$ ) and 2) able to isolate the furnace chamber thermally.

NOTE: The resulting temperatures of the window may influence the window transmission.

1.5.3.2. Avoid damage of the IR window. Do not tighten the window into a structure, which helps to avoid overpressure during material expansion.

NOTE: The window material should have a sufficient amount of space to expand when heated up.

1.6. Check the resulting field of view (FOV) of the IR camera by examining the thermography image via the IR camera software. Identify the targeted object and its temperature in the thermography image. Adjust the FOV, if necessary.

## **2. Uniform customer temperature correction of a fabrication calibrated IR camera**

CAUTION: The fabrication of the IR camera is assumed to include a radiometric calibration.

2.1. Spot local optical artifacts, such as reflection and background radiation.

2.2. Conduct classic thermocouple measurements of the object while simultaneously recording the wafer including thermocouple with the IR camera.

2.2.1. Check the validity of the used thermocouples. Search for known characteristic temperature points in the temperature profile of the processed object that can be clearly visibly detected (e.g., disruption in a smooth line). If the thermocouple measures these temperature points correctly, the thermocouple is most likely correctly calibrated.

### **2.2.2. Example using silicon solar cells**

2.2.2.1. Place the thermocouple on the rear aluminum side of the wafer. Take a temperature profile for a standard firing process<sup>11</sup>.

2.2.2.2. Validate the thermocouples by determining whether there is a disruption in the temperature profile from step 2.2.2.1 around the Al-Si eutectic temperature of 577 °C in the form of a flatter curve (as is the case in **Figure 2D**).

NOTE: If the disruption occurs at the temperature around 577 °C, it is a sign that the temperature measurement by the thermocouple is accurate. Use only validated thermocouples for the following steps.

2.2.3. Conduct thermocouple measurements in the temperature range of interest at the same object spot (multiple times for statistical reasons), then at spatially various random spots (for statistical reasons) to obtain time-temperature profiles.

2.3. Determine the local uncorrected thermography object temperature underneath the thermocouples from the thermocouple measurements from step 2.2.3.

2.3.1. Check for a possible local temperature drop around the contacting thermocouple (due to heat dissipation and shading). Assume the temperature in the vicinity of the thermocouple as the object temperature directly under the thermocouple, if a local temperature drop is not present.

2.3.2. Perform the following steps if a local temperature drop is present.

2.3.2.1. Determine the spatial temperature gradient of the present temperature drop in the part that is not covered by the thermocouple.

NOTE: It is recommended to determine the gradient at multiple spots around the temperature drop (radially) and form an average gradient.

2.3.2.2. Estimate the contribution of possible optical artifacts induced by the thermocouple (example protocol for a case in which homogenous temperature along the cell depth direction is assumed, such as in Si solar cells).

2.3.2.2.1. Place the thermocouple on the surface opposite to the measured surface and repeat the thermocouple and thermography measurement in this configuration (as shown in **Figure 3A**). Turn the object, including the thermocouple, around so that the thermocouple is not in the optical path between the camera and object.

NOTE: If the gradient of the local temperature drop is the same for the thermocouple being inside and outside of the optical path (i.e., attached to the measured or opposite surface), it is a sign that the thermocouple most likely does not induce optical artifacts.

2.3.2.2.2. Extrapolate the gradient of the temperature drop in the case of the thermocouple contacting the measured surface (i.e., inside optical path) to the area covered by the thermocouple to obtain the temperature of the object underneath the thermocouple.

2.3.2.2.3. Repeat 2.3.2.2.2 for each measurement from step 2.2.3.

2.4. Correct the uncorrected thermography image with respect to the thermocouple measured temperatures with the data generated from steps 2.2.3 and 2.3.2.2.3.

2.4.1. Plot the measured temperatures via thermocouples against the determined temperatures via uncorrected IR thermography. Conduct a curve fitting.

2.4.2. Apply the obtained curve fit as a general uniform global correction formula for the uncorrected thermography image.

2.5. Repeat the temperature correction for each new object type or configuration, especially

when the optical parameters differ.

### 3. Evaluation of spatial surface temperature distribution via IR thermography

NOTE: The firing conditions are assumed to be identical for this section.

#### 3.1. Temperature distribution opposite to throughput direction (see red arrow in **Figure 4A**)

3.1.1. Conduct multiple line scans of the object temperature (e.g., with the software ImageJ) opposite to the throughput direction (indicated in the inset picture of **Figure 4A**).

3.1.2. Average the line scans in throughput direction in order to get one average line scan in the direction opposite to the throughput direction. This average line scan represents the surface temperature distribution of the object in the direction opposite to the throughput direction.

#### 3.2. Temperature distribution parallel to throughput direction (**Figure 4B**)

3.2.1. Choose multiple fixed positions in the furnace (indicated in inset picture of **Figure 4B**).

3.2.2. Scan the temperature of the passing object from the heading to trailing edge.

3.2.3. Convert the temporal distribution to spatial distribution (linear conversion for assumed constant velocity).

3.2.4. Average all the temperature distributions in perpendicular throughput direction in order to get the averaged distribution in throughput direction. This average distribution represents the surface temperature distribution of the object in the throughput direction.

#### 3.3. Creation of a 2D temperature distribution map (**Figure 4C**)

3.3.1. Track the surface object temperature for each object surface spot along the entire camera FOV.

3.3.2. Calculate the maximum value for each object spot and plot the maximum values of each position in a 2D distribution map.

### REPRESENTATIVE RESULTS:

As shown in **Figure 3B–D**, the example object (here, a silicon solar cell; strictly speaking, a passivated emitter and rear cell [PERC]<sup>12</sup>; **Figure 2A,B**) can be clearly detected by the IR camera in different configurations<sup>4</sup>. The different configurations are monofacially metallized (**Figure 3B**), bifacially metallized<sup>13</sup> (**Figure 3C**) and nonmetallized PERC cells (**Figure 3D**). The difference between the monofacial and bifacial configuration is that the former has a full area aluminum layer, whereas the latter has an H-pattern grid (similar to the silver front side) on the rear side. Here, the IR camera was positioned in a way that the camera FOV captured the peak temperature



of the firing process. The peak phase is the most crucial phase during the firing process, since the contacts are actually formed during this phase<sup>14</sup>. Here, the temperature range of interest resembled the typical peak temperature range of the firing process (i.e., ca. 700–900 °C<sup>1</sup>).

For the latter temperature range, the spectral emissivity is quite high and homogenous in the short, middle, and long wavelength infrared spectra<sup>3</sup>. A double sapphire layer was used as a transmissive window, allowing for good transmission in the short and middle IR wavelength spectra. In order to minimize detection of light from the IR lamps of the furnace (peak wavelength in short wavelength infrared range), an IR camera type with InSb as detector material was chosen, with a detection range of 3.7–4.1 μm (including filters). Only one-third of the wafer in the throughput direction can be detected at the same time. However, it was sufficient for this work, since each wafer position can be detected at a fixed furnace position. Naturally, temperature corrected thermography images are shown here. Strictly speaking, the image is temperature-corrected with respect to the solar cells.

As can be seen in **Figure 3A**, the contacting thermocouple on the opposite side of the optical path caused a temperature drop around itself (with a temperature drop of 10 K), most likely due to heat dissipation and shading. The latter drop is important to estimate the cell temperature during firing without thermocouples, compared to the temperature measured by the thermocouple. Here, the cell was positioned onto a frame when contacted by a thermocouple (**Figure 3E**). The heat dissipation by the frame caused a temperature drop of around 10 K. Together with the additional heat drop by the thermocouple, the latter measured a 20 K lower temperature than what the cells displayed during standard processing (without the thermocouple equipment). It is important to estimate the latter offset for the used thermocouple system, which is performed with the help of thermography, as shown. The IR camera allows observation of the local heat dissipation of the cells by the conveyor belt if placed directly on the belt (**Figure 3F**). This is the reason why cells are usually placed on belt elevations to minimize contact between them and the belt.

**Figure 4** shows the surface temperature distribution. Since silicon solar cells are typically around 160 μm thick and processed in the furnace for 30 s, it is likely that the temperature distribution along the cell depth is homogenous. Therefore, the results most likely suggest a temperature distribution rather than only a surface temperature distribution. Opposite to the throughput direction, an average temperature gradient of 1 K/cm was obtained. In the throughput direction, the incoming wafer quarter was substantially colder than the trailing wafer rest. The colder incoming portion experienced a gradient of 7 K/cm, while the hotter trailing part experienced a gradient of 0.5 K/cm.

In both directions, the cell edges (the remaining 2 cm) were ignored for determination of the gradients, since the detected temperature at the edges mixed with the colder outside boundary of the cells, resulting in false temperatures. **Figure 4C** shows a representative 2D temperature distribution of a monofacial solar cell, which was not metallized at the front side. The abovementioned trends in the same and opposite transport directions were observed here, as well. All in all, these results reveal that the solar cells in this work experienced a certain degree

of spatial temperature inhomogeneity.

#### FIGURE LEGENDS:

**Figure 1: Most important equipment used in the protocol.** (A) Lateral scheme of the conveyor belt furnace. This figure panel has been modified from Ourinson et al.<sup>4</sup>. (B) Zoomed-in last firing zone, visualizing the setup of the thermography system. 1) Furnace wall and isolation, 2) IR camera, 3) IR lamps, 4) insulating window, 5) object transport direction, 6) camera FOV, 7) transportation belt, 8) object, and 9) thermography software. This figure panel has been modified from Ourinson et al.<sup>4</sup>. (C) The firing furnace used during this protocol. (D) Image illustrating the used IR camera and transmissive IR window positioned in the firing furnace. The numbers correspond to the numbers from panels A and B.

**Figure 2: Measured objects and their temperatures.** (A) Schematic cross-section of a monofacial PERC solar cell. (B) Front (left) and rear (right) side view of an industrial PERC cell. (C) Thermocouple-measured industrial time-temperature profile of a PERC solar cell during the firing process, including segmentation into phases and section, which is covered by the camera field of view. This figure has been modified from Ourinson et al.<sup>5</sup>. (D) Demonstration of disruption around the eutectic temperature ( $T_{EUT}$ ) of aluminium and silicon in a firing profile measured by a thermocouple, when the thermocouple is placed on the aluminium rear side of the solar cell. This figure has been modified from Ourinson et al.<sup>5</sup>.

**Figure 3: Representative temperature-corrected thermography images of PERC solar cells for identical firing conditions.** (A) Visible local temperature drop caused by contact of a thermocouple from the rear side. (B) Thermography image of the upper one-third of a monofacially metallized PERC cell, including (1) visible busbars (2) positioned on the visible conveyor belt.  $T_{AV}$  shows the average temperature on the wafer. (C) Thermography image of a bifacially metallized PERC cell. (D) Thermography image of a nonmetallized PERC wafer. (E) Thermography image of a wafer placed on a thermocouple frame and contacted by a thermocouple.  $T_{TC}$  shows the wafer temperature measured by the thermocouple. (F) Thermography image of a wafer placed directly on the conveyor belt. (G) Color map of the temperature range measured by the IR camera. This figure has been modified from Ourinson et al.<sup>5</sup>.

**Figure 4: Temperature distribution of a PERC solar cell for identical firing conditions.** (A) Temperature distribution in perpendicular direction to the throughput direction. Black thin curves present the temperature distribution along the line scans, which are shown in the inset pictures. The green bold curve presents the temperature distribution, which is the average of the temperatures shown by the thin black curves. This figure panel has been modified from Ourinson et al.<sup>4</sup>. (B) Temperature distribution in the throughput direction. Black thin curves present the temperature distribution recorded by the fixed furnace positions, which are shown in the inset picture. The green bold curve represents the average of the temperatures shown by the black thin curves. This figure panel has been modified from Ourinson et al.<sup>4</sup>. (C) 2D temperature distribution of the maximum temperature of a passing monofacial solar wafer, which is not metallized at the front side. The conveyor belt is visible at the left and right corners, as well.

## DISCUSSION:

Commonly, thermography temperature is corrected via measuring and adapting the optical parameters of the object, transmissive window and path, and environmental temperature of the object and transmissive window<sup>2</sup>. As an alternative method, a temperature correction technique based on thermocouple measurements is described in this protocol. For the latter method, knowledge of the parameters mentioned above is not required. For the application shown here, this method is sufficient. However, it cannot be guaranteed that the thermocouple method is sufficient for all thermography applications in a conveyor belt furnace.

In the protocol, a uniform global temperature correction of the thermography image is proposed; although, it is more precise to correct the spatially resolved temperature. However, it has been found that the uniform temperature correction is more appropriate in cases of moving objects. Furthermore, it is intended to correct the temperature of the object rather than the surrounding objects (e.g., the belt and walls).

As mentioned in step 2.3.3.2, the example provided here is assumed to have a homogeneous temperature distribution along the object depth. In cases of objects with inhomogeneous temperature distribution along their depths, the temperature on one surface does not resemble the temperature on the opposite surface. Thus, the steps described in section 2.3.3.4 do not apply for these cases. A solution for inhomogeneous temperature distribution along the object depth must be further studied.

## ACKNOWLEDGMENTS:

This work is supported by the German Federal Ministry for Economic Affairs within the project “Feuerdrache” (0324205B). The authors thank the co-workers that contributed to this work and the project partners (InfraTec, Rehm Thermal Systems, Heraeus Noblelight, Trumpf Photonic Components) for co-financing and providing outstanding support.

## DISCLOSURES:

The authors have nothing to disclose.

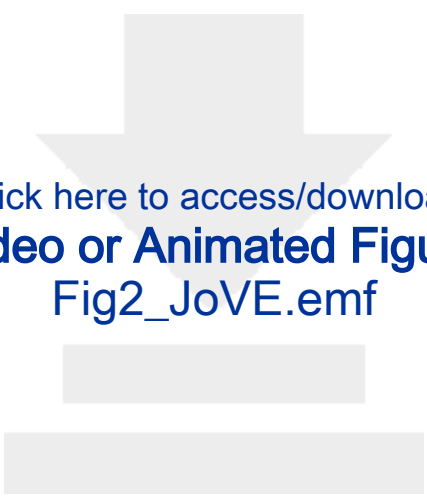
## REFERENCES:

1. Xu, J., Zhang, J., Kuang, K. *Conveyor Belt Furnace Thermal Processing*. Springer. Heidelberg, Germany (2018).
2. Breitenstein, O., Warta M. W. Langenkamp *Lock-in Thermography: Basics and Use for Evaluating Electronic Devices and Materials*. Springer. Heidelberg, Germany (2010).
3. Ravindra, N. M., Ravindra, K., Mahendra, S., Sopori, B., Fiory, A. T. Modeling and Simulation of Emissivity of Silicon-Related Materials and Structures. *Journal of Electronic Materials*. **32** (10), 1052–1058 (2003).
4. Ourinson, D. et al. In Situ Solar Wafer Temperature Measurement during Firing Process via Inline IR Thermography. *Physica Status Solidi (RRL) - Rapid Research Letters*. **13** (10), 1900270 (2019).

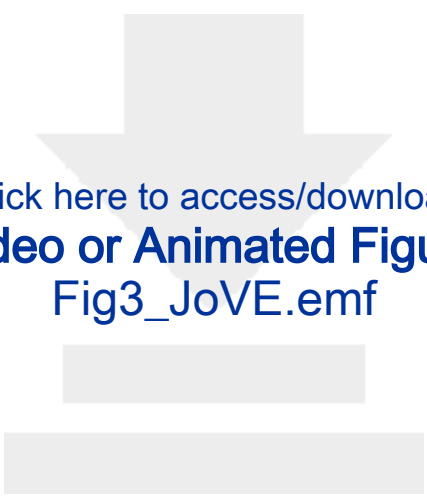
5. Ourinson, D. et al. In-situ wafer temperature measurement during firing process via inline infrared thermography *AIP Conference Proceedings*. **2156**, 020013 (2019).
6. Cooper, I. B. et al. Understanding and Use of IR Belt Furnace for Rapid Thermal Firing of Screen-Printed Contacts to Si Solar Cells. *IEEE Electron Device Letters*. **31** (5), 461–463 (2010).
7. Schubert, G., Huster, F., Fath, P. Physical understanding of printed thick-film front contacts of crystalline Si solar cells—Review of existing models and recent developments. *Solar Energy Materials and Solar Cells*. **90** (18–19), 3399–3406 (2006).
8. Rauer, M. et al. Aluminum Alloying in Local Contact Areas on Dielectrically Passivated Rear Surfaces of Silicon Solar Cells. *IEEE Electron Device Letters*. **32** (7), 916–918 (2011).
9. Pawlik, M., Vilmot, J. -P., Halbwax, M., Gauthier, M., Le Quang, N. Impact of the firing step on Al<sub>2</sub>O<sub>3</sub> passivation on p-type Czochralski Si wafers: Electrical and chemical approaches. *Japanese Journal of Applied Physics*. **54** (8S1), 08KD21 (2015).
10. Lee, B. J., Zhang, Z. M. RAD-PRO: Effective Software for Modeling Radiative Properties in Rapid Thermal Processing. *2005 13th International Conference on Advanced Thermal Processing of Semiconductors*. Santa Barbara, CA (2005).
11. Temperature Measurements. <https://meettechniek.info/measuring/temperature.html> (2020).
12. Blakers, A. W., Wang, A., Milne, A. M., Zhao, J., Green, M. A. 22.8% efficient silicon solar cell. *Applied Physics Letters*. **55** (13), 1363–1365 (1989).
13. Dullweber, T. et al. PERC+: industrial PERC solar cells with rear Al grid enabling bifaciality and reduced Al paste consumption. *Progress in Photovoltaics: Research and Applications*. **24** (12), 1487–1498 (2016).
14. Ourinson, D., Emanuel, G., Lorenz, A., Clement, F., Glunz, S. W. Evaluation of the burnout phase of the contact firing process for industrial PERC. *AIP Conference Proceedings*. **2147** (1), 040015 (2019).








Click here to access/download  
**Video or Animated Figure**  
Fig2\_JoVE.emf



Click here to access/download  
**Video or Animated Figure**  
Fig3\_JoVE.emf





Click here to access/download  
**Video or Animated Figure**  
Fig4\_JoVE.emf

Name of Material/Equipment	Company	Catalog Number	Comments/Description
Datalogger incl. Thermal barrier	Datapaq Ltd.		
IR thermography camera "Image IR 8300"	InfraTec GmbH		
IR thermography software "IRBIS Professional 3.1"	InfraTec GmbH		
Solar cells	Fraunhofer ISE Rehm Thermal		
Solar firing furnace "RFS 250 Plus"	Systems GmbH		
Sheath thermocouples type K	TMH GmbH Heraeus		
Thermocouple quartzframe	Noblelight GmbH		

Dear Editor,

Thank you very much for the further review of our paper. All your comments have been addressed. Please find the responses in the following text and in the marked version of the manuscript. We hope that we have met your expectations. We are not sure, whether you removed the yellow highlighting in the first chapter of the protocol section on purpose or by accident, which is why we put back the highlighted parts as they were when submitted last time. If you deliberately deleted those the highlighting, we will accept it, though.

Best regards,  
Daniel Ourinson

“Do you mean the burnout area or the firing area shown in Figure 1A?”

Yes, the sentence has been changed.

“Wavelength range(s) **of** the highest emission?”

It has been replaced accordingly.

“Please provide these parameters for the silicon solar cell tested. Such information can be included in a “NOTE” below this step.”

The information has been added.

“How?”

After reading the original sentence, we think we did not formulate the task well. Now it should be clearer.

“Does the size matter here? Please specify the size of the wafer. We need specific details of the sample so this protocol can be reproduced.”

Size does not matter here, as it has been inserted into the sentence now. This is why the size was not specified.

“Please add a reference to published material specifying how to perform this.”

Done.

“Do you mean thermocouple measurements?”

Yes, it has been changed.

“Do you obtain a time-temperature profile (e.g., Figure 2C,D) after this step? Please specify what data is generated from this step.”

Yes, it has been changed.

“Check what?”

Unfortunately we do not understand this question. It says here clearly that a possible local temperature drop should be checked for.

“How?”

This work is not about teaching how to take general gradients. We assume that the interested readers will know how to perform this. But for clarification that we talk here about spatial gradients the word “spatial” has been inserted here.

“Do you mean the direction indicated with the red arrow?”

Yes, the sentence has been clarified.

“Should not step 3.1 start with IR thermography as described in steps 3.2.1 and 3.2.2?”

No, because the object is only moving in throughput direction not opposite to it. This is why different approaches, as described are necessary.

“ImageJ is an image processing program. Do you analyze raw data (i.e., temperature) generated by IR thermography here?”

Yes.

“What do line scans represent here?”

Line scans of the object temperature. The sentence has been changed accordingly.



RE: Copyright of my own articleAIPRights Permissions An:

daniel.ourinson@ise.fraunhofer.de 31.10.2019 15:50

Von: "AIPRights Permissions" <Rights@aip.org>

An: "daniel.ourinson@ise.fraunhofer.de" <daniel.ourinson@ise.fraunhofer.de>

Dear Dr. Ourinson:

Thank you for requesting permission to reproduce material from AIP Publishing publications.

Material to be reproduced:

Figures from:

AIP Conference Proceedings 2156, 020013 (2019); <https://doi.org/10.1063/1.5125878>

For use in the following manner:

Reproduced in a new work.

Permission is granted subject to these conditions:

1. AIP Publishing grants you non-exclusive world rights in all languages and media. This permission extends to all subsequent and future editions of the new work.

2. The following notice must appear with the material (please fill in the citation information):

“Reproduced from [FULL CITATION], with the permission of AIP Publishing.”

The notice may appear in the figure caption or in a footnote. In cases where the new publication is licensed under a Creative Commons license, the full notice as stated above must be used.

3. If the material is published in electronic format, we ask that a link be created pointing back to the abstract of the article on the journal website using the article’s DOI.

4. This permission does not apply to any materials credited to another source.

Please let us know if you have any questions.

Sincerely,

**Susann LoFaso**

*Manager, Rights & Permissions*

**AIP Publishing**

1305 Walt Whitman Road | Suite 300 | Melville NY 11747-4300 | USA

t +1.516.576.2268

[rights@aip.org](mailto:rights@aip.org) | [publishing.aip.org](http://publishing.aip.org)

Follow us: [Facebook](#) | [Twitter](#) | [LinkedIn](#)

**From:** daniel.ourinson@ise.fraunhofer.de <daniel.ourinson@ise.fraunhofer.de>

**Sent:** Wednesday, October 30, 2019 11:11 AM

**To:** AIPRights Permissions <Rights@aip.org>

**Subject:** Copyright of my own article

Dear Sir or Madam,

I want to reuse my own graphs of the article "

# **In-situ wafer temperature measurement during firing process via inline infrared thermography"**

which is published in the AIP proceedings. Do I need a copyright license for this? Does it cost money, even though it's my own article and graphs?

Thank you very much for your help!

Best regards,  
Daniel Ourinson

--

Daniel Ourinson, M.Sc.  
Department "Production Technology - Structuring and Metallization"  
Division Photovoltaics  
Fraunhofer Institute for Solar Energy Systems (ISE)  
Heidenhofstrasse 2, 79110 Freiburg, Germany  
Phone: +49 761 4588 - 5058  
[daniel.ourinson@ise.fraunhofer.de](mailto:daniel.ourinson@ise.fraunhofer.de)  
[www.ise.fraunhofer.de](http://www.ise.fraunhofer.de)

Dear Daniel Ourinson,

**Physica Status Solidi (RRL) Rapid Research Letters**

**"In-situ Solar Wafer Temperature Measurement During Firing Process Via Inline Infrared**

**Thermography OPEN"**

**Article DOI: 10.1002/pssr.201900270**

Thank you for your recent communication regarding the use of your article for dissertation.

Our copyright policy allows researchers to self-archive the submitted and accepted version of an article on their own personal website, in a company/institutional repository or archive, and in approved not-for-profit subject-based repositories after an embargo period.

However, our policy does not currently permit the public posting of any version of the article (submitted, accepted or final) to such scholarly networks. More information on our policy about this can be found at: <http://olabout.wiley.com/WileyCDA/Section/id-820227.html>

For your convenience, we have also attached a copy of your article along with the terms and conditions of article use.

**e-Offprint Terms & Conditions**

The following Terms and Conditions relate to the use of this e-Offprint file. Use of this e-Offprint file indicates consent to these Terms and Conditions.

Provided that you give appropriate acknowledgement to the Journal, Association/Society and the publisher, and give full bibliographic reference for the Article, and as long as you do not sell or reproduce the Article or any part of it for commercial purposes (i.e. for monetary gain on your own account or on that of a third party, or for indirect financial gain by a commercial entity) you may use the PDF, in the following ways:

- You have the personal right to send or transmit individual copies of this PDF to colleagues upon their specific request provided no fee is charged, and further-provided that there is no systematic distribution of the Contribution, e.g. posting on a listserv, website or automated delivery.
- You have the personal right to include this PDF in teaching or training duties at your institution/place of employment including in course packs, e-reserves, presentation at professional conferences, in-house training, or distance learning. Except by separate agreement, this PDF may not be used in seminars outside of normal teaching obligations (e.g. commercial seminars). Electronic posting of the final published version in connection with teaching/training at your institution/place of employment is permitted subject to the implementation of reasonable access control mechanisms, such as user name and password.

Please note that you are not permitted to post the Wiley PDF version of the Article online unless you have paid the OnlineOpen fee.

For additional information regarding any use of this PDF file not covered by these Terms and Conditions, please refer to the Wiley Rights Department at: [jrights@wiley.com](mailto:jrights@wiley.com). We hope this information helps.

Please do not hesitate to contact us if you require further assistance.

Kind regards,

**Richard Jonathan Chua**  
Wiley Author Support



If you require further assistance with this matter or would like answers to frequently asked questions, please visit [Wiley Author Support](#), 24 hours a day, 7 days a week.

Subject     Reuse of Figures

Dear Sir or Madam,

I want to reuse my own graphs of the article "In Situ Solar Wafer Temperature Measurement during Firing Process via Inline IR Thermography" which is published in PSS RRL. Do I need a copyright license for this? I tried to fill out one form, and it resulted in a payment of 1300 USD. I cannot believe that is the right way. Do I even need a copy right if it is my own paper and my own figures?  
Thank you very much for your help!